Regioselectivity of the coupling between radicals and ambident nucleophiles. A theoretical study†

María T. Baumgartner,* Guillermo A. Blanco and Adriana B. Pierini

Received (in Gainesville, FL, USA) 18th July 2007, Accepted 25th October 2007
First published as an Advance Article on the web 12th November 2007
DOI: 10.1039/b710998a

We here report a theoretical study on the reaction of the anions of phenol, 2-naphthol, the pyrimidine bases (uracil, thymine, cytosine), pyrrole, imidazole and benzimidazole with phenyl and 4-nitrobenzyl radicals with the aim of interpreting the factors that control the regiochemical outcome of these reactions; their main features being C–C bond formation with phenyl radicals and C–heteroatom bond formation with 4-nitrobenzyl radicals. The preferred coupling positions were investigated by evaluation of the frontier molecular orbital theory (FMO) indexes and the potential energy surfaces both at the AM1 and DFT/B3LYP levels. Within the latter methodology, the solvent effect was considered under a continuum model. While FMO predicts the experimental regioselectivity of phenyl radicals with good accuracy, it fails in the nitrobenzyl case. On the other hand, studies of transition state stabilities provide a good prediction of the observed regioselectivity for both types of radicals, mainly when the solvent is taken into account.

Introduction

As it is well known, radicals are highly reactive species which react by different mechanistic pathways. One of these paths, of relevance in synthetic organic chemistry, is the coupling with an anion to form a radical anion. This is one of the key steps of the $S_{RN}1$ mechanism through which a nucleophilic substitution, mediated by electron transfer (ET), can be achieved on aromatic and aliphatic halides that, due to steric, geometric or electronic factors, are poorly reactive through classical polar processes.[1]

In the $S_{RN}1$ mechanism (Scheme 1), the radicals can be formed either by a two-step (eqn (1) and (2)), or by a concerted one-step (eqn (1) + (2)) ET from an adequate electron source to the substrate (RX, R = alkyl, aryl). The radicals formed react with the nucleophile (Nu^-) present in the reaction media to form the radical anion $RNu^{-\bullet}$ (eqn (3)) which, by ET to the substrate (eqn (4)), affords the substitution product and the intermediate that propagate the cyclic process.

Different anions have been shown to react by this means. Anions from P, S, Sn, As, Sb, Se and Te react through the heteroatom to form a C–heteroatom bond.[1] The anions from ketones, esters, amides and thioamides, nitroalkanes, nitriles, and mono and dianions from β-dicarbonyl compounds react at their carbon site to form a C–C bond.[1]

An ambident coupling behaviour has been observed with anions such as ArO^-, $ArNH^-$ and heteroaryl nitrogen nucleophiles. Phenoxide ions react with aromatic radicals at their *ortho* or *para* carbons (eqn (5a)) and C_1 arylation is the main reaction of 2-naphthoxide anion with aromatic radicals. Following this route, different hydroxybiaryls have been synthesised in good yields.[2–4] On the other hand, an efficient O-alkylation occurs in the $S_{RN}1$ reaction of *p*-nitrocumyl radicals with 1-methyl-2-naphthoxide[5] and phenoxide ions (eqn (5b)).[6]

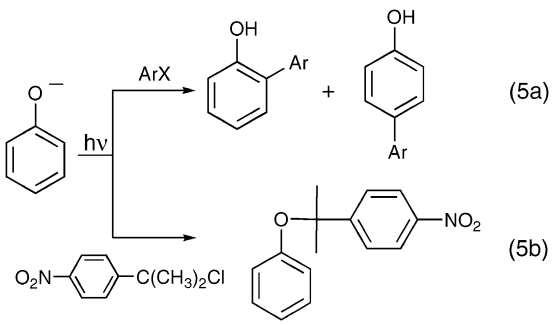

A similar regiochemical pattern has been found in the reaction of $ArNH^-$ and heteroaryl nitrogen anions which show a preference for C-arylation with aryl[7,8] and perfluoroalkyl radicals[9] (eqn (6a)). Thus, aminobiaryls have been synthesised in good yields in the photo-initiated reaction of haloarenes

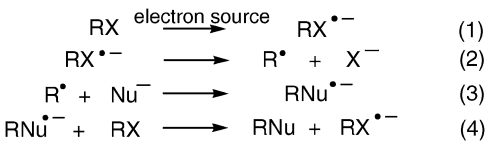

Scheme 1

INFIQC, Departamento de Química Orgánica, Facultad de Ciencias Químicas. Universidad Nacional de Córdoba, Ciudad Universitaria, 5000 Córdoba, Argentina. E-mail: tere@fcq.unc.edu.ar; Fax: +54-351-4333030/4334170; Tel: +54-351-4334170/73

† Electronic supplementary information (ESI) available: The AM1 conformational search for RAs formed by reaction of phenyl radical (**10**) at the C1 and O sites of anion **2**. ΔEsolvation (kcal mol^{-1}) in methanol for the coupling of aromatic and alipahtic radicals with the nucleophiles of Chart 1. Electrostatic potential and spin distribution for RAs and TSs formed by reaction of anion **1** with radicals **11**, **12**, and anion **2** with radical **10**. Charge distribution of RAs for the coupling of anions (**1**, **5** and **8**) at heteroatom and C positions with phenyl radical. The AM1 SOMO for RAs. Energy differences between relevant points of the potential energy surface (PES) for the reaction of phenyl radicals (**10**) with anion **2** calculated with different bases. See DOI: 10.1039/b710998a

with arylamide anions.[7,8] Arylpyrroles, arylindoles and arylimidazoles have also been obtained by reaction of aromatic compounds with the corresponding heteroaryl nitrogen anions.[9–11] A preference for heteroatom (*N*)-alkylation has been reported in the reaction of these anions with alkyl radicals substituted by π-electron withdrawing groups (EWG) (eqn (6b)).[12]

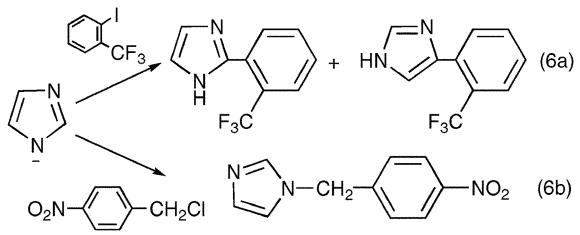

In terms of driving force, the factors governing the coupling with a given anion depend on the strength of the bond being formed in the new radical anion $(RNu)^{-\bullet}$, and on the standard potential for its oxidation ($E^{\circ}_{RNu^{-\bullet}/RNu}$) or the reduction potential of the neutral. For example, the exclusive α-C coupling obtained with the enolate anions of ketones has been explained in terms of a strong driving force advantage for C–C over C–O bond formation with bond strengths of 4.18 and 3.05 eV, respectively. Moreover, the reduction potential of the product formed by C–C coupling is more positive than that of the product formed by C–O coupling.[13]

There is no definitive bond strength advantage for C- over O-coupling for phenyl radicals with PhO^{-} (3.30 eV and 3.38 eV, respectively).[13] However, the reduction potential of the product from C–C coupling is expected to be positive with respect to the C–O product and therefore, the C–C route is estimated to be preferred, but not to a large extent. On the other hand, an aryloxy substituent attached to an α-benzylic carbon is expected to exert a lesser effect on the stability of a radical anion and on the reduction potential of the neutral than when directly attached to an aromatic carbon, and no clear factors emerge to explain the regiochemistry of these anions with activated benzylic radicals.[13] For this reason we consider it appropriate to perform a theoretical study of the selectivity of the coupling with the wide range of anions presented in Chart 1 (the numbering of the coupling positions is shown).

Phenyl and 4-nitrobenzyl radicals were chosen as representative of the aromatic and aliphatic activated radical series, respectively.

The evaluation of the topological static indexes corresponding to a radical–anion coupling within the FMO theory was the simplest theoretical approach used. Besides, the potential energy surfaces (PESs) of the reactions were examined with the semiempirical AM1 method as well as within the DFT theory and the B3LYP functional. In these calculations, the solvent effect was also modelled.

Results and discussion

Within FMO, the stabilisation corresponding to the coupling of a given radical at different sites of a nucleophile can be evaluated by the interaction of the SOMO of the radical and

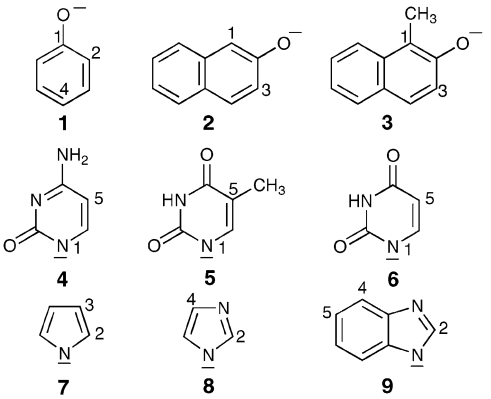

Anions of: phenol (**1**), 2-naphthol (**2**), 1-methyl-2-naphthol (**3**), cytosine (**4**), tymine (**5**), uracil (**6**), pyrrole (**7**), imidazole (**8**), benzimidazole (**9**).

Radicals: phenyl (**10**), 4-nitrobenzyl (**11**)

Chart 1

the HOMO of the anion. In all the cases here reported, the energy of the HOMO of the nucleophiles is higher than the energy of the SOMO of the radicals. In consequence, the stabilisation energy from the FMO theory is calculated according to eqn (7).[14]

$$\Delta E = \varepsilon'' + (E_{HOMO} - E_{SOMO}),\ \varepsilon'' = (c_{Hi}c_{Sj}\beta_{ij})^2/(E_{HOMO} - E_{SOMO}) \quad (7)$$

As the HOMO − SOMO energy difference ($E_{HOMO} - E_{SOMO}$) remains constant for a given radical–nucleophile pair, the preferred reaction site for a given anion can be directly estimated from the second order perturbation ε'', and consequently, the preferred site will be the atom bearing the largest HOMO coefficient.[15]

The HOMO and SOMO energy, the coefficients of relevance and the ε'' evaluated for the equilibrium geometries of each reactive pair are presented in Table 1 for nucleophiles **1–9** and phenyl (**10**) and 4-nitrobenzyl (**11**) radicals.

The PESs corresponding to C–C and C–heteroatom bond formation (eqn (8a) and (8b), respectively, for anion **2** as representative) were inspected starting from the most stable conformer of the radical anions formed at the relevant sites of each anion.

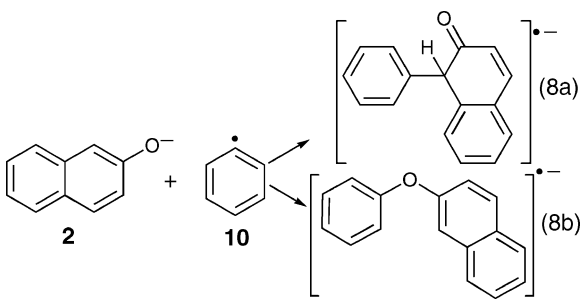

The degrees of freedom of these intermediates are limited, and the search of conformational space is further simplified (see

Table 1 AM1 HOMO and SOMO energies, c_{Hi} and c_{Sj} coefficients, and second order perturbation (ε'') at different reactive sites of anions **1–9**

Anion	Position	HOMO/eV	c_{Hi}	ε'' with **10**[a]	ε'' with **11**[a]
1	C_2	−2.702	0.476	**0.468**	0.372
	C_4		0.548	**0.622**	0.493
	O		0.459	0.248	**0.196**
2	C_1	−3.036	0.578	**0.723**	
	C_3		0.275	0.163	
	O		0.407	0.204	
3	C_1	−3.000	0.587	0.742	0.591
	C_3		0.260	0.146	0.116
	O		0.397	0.193	**0.154**
4	C_5	−3.692	0.644	0.986	
	N_1		0.445	0.357	
5	C_5	−4.038	0.688	1.188	0.945
	N_1		0.541	0.558	**0.442**
6	C_5	−3.926	0.680	**1.140**	
	N_1		0.511	0.487	
7	C_2	−2.551	0.601	**0.732**	
	C_3		0.374	0.284	
	N		0.001	0.000	
8	C_2	−2.923	0.603	**0.776**	0.617
	C_4		0.537	**0.615**	0.489
	N		0.171	0.047	**0.038**
9	C_2	−3.764	0.026	0.002	0.001
	C_4 (7)		0.395	0.376	0.303
	C_5 (6)		0.306	0.225	0.181
	N		0.508	**0.470**	**0.379**

Radical	SOMO/eV	c_{Sj}
10	−10.243	0.790
11	−9.546	0.670

[a] Experimental preferred reaction sites for a given anion with phenyl (**10**) or 4-nitrobenzyl (**11**) radicals indicated in bold.

ESI, Fig. S1†). Table 2 and Table 3 collect the difference in energy between the critical structures located along the PESs for the reaction of radicals **10** and **11** with anions **1–9**. The gas phase minimum PESs evaluated either by AM1 or B3LYP show a similar profile for all systems; the formation of the carbon or heteroatom radical anion (eqn (8a) and (8b), respectively) being an exothermic reaction.

Phenyl radical (10)

As seen from Table 1, the second order perturbations evaluated for the reaction of the anions with **10** reinforces the selectivity shown by the HOMO coefficients.[15] The relative reactivity order predicted by FMO for the oxyanion family is: $C_4 > C_2 > O$ for anion **1** and $C_1 > O > C_3$ for anions **2** and **3**.

The order for the heteroaryl nitrogen anions series is: $C_5 > N_1$ for **4**, **5** and **6**; $C_2 > C_3 \gg N$ for **7** (null at N); $C_2 > C_4 \gg N$ for **8** (almost null at N), and $N > C_4$ for **9**.

As can be seen, C–C bond formation is predicted as the preferred reaction pathway of **10** with all the anions under consideration, except **9**.

This reactivity pattern is in agreement with the experimental outcome of the reactions. Thus, in the oxyanion family anion **1** has been reported to react with aryl radicals to afford products only from C_{para} ($\approx$20%) and C_{ortho} ($\approx$40%) coupling;[3,16] the preferred C_{ortho} substitution being ascribed to a statistically higher probability for the *ortho* site with respect to the *para* one. Arylation at C_1 (>40%) was the only informed product for the reaction of **2** with different aryl halides;[2] similar results are predicted for **3**, for which no experimental information with aromatic radicals is available.

Within the heteroaryl nitrogen series C_5-arylation has been the only product reported in the reaction of uracil anion **6** with aryl halides.[17] Similarly, C_2-phenylation (60%) accompanied by a low yield of C_3-coupling (7%) has been observed for the reaction of pyrrole anion **7** with phenyl radicals.[9] Imidazole anion **8** reacts with aromatic radicals to afford the products from coupling at C_2 and C_4; the yield of reaction at C_4 being higher than that at C_2 (with phenyl radical[10] $C_4/C_2 = 4$ and with perfluoroalkyl radicals[11] $C_4/C_2 \approx 2$ or 1).

The experimental information for anion **9** is scarce and only N-substitution has been reported, although in low overall yields.[18]

In Fig. 1–3, the AM1 and B3LYP PESs evaluated for the reaction of radical **10** at the different relevant sites of anions **2**, **6** and **7**, taken as representative of each family, are presented, respectively. As shown in the figures, the gas phase PES exploration shows the exothermic coupling reaction usually taking place with low or no activation energy.

For oxyanions **1–3** (Table 2), the energy barriers for O-coupling are the highest by either method. Reaction at C_1 of **2** is the preferred energy path affording the most stable C_1 intermediate ($\approx$15 kcal mol^{-1} lower in energy than the O-radical anion). A similar profile is obtained for coupling at C_3 of **3** (Table 2). For this anion the different outcome obtained by FMO (C_1 preferred) and PES is attributed to steric constraints for reaction at C_1 which are only accounted for by PES studies.

Similar PES profiles were obtained with AM1 for the three pyrimidine anions **4–6**, and with B3LYP and AM1 for **6** (see Fig. 2).

The reaction at C_5 is the route with the lower energy barrier for anions **4–6** (see Table 2). Coupling at this position of **5** and **6** affords the most stable radical anion. No experimental information is available for anions **4** and **5**.

Even though FMO, AM1 and B3LYP predict the C-coupling as the kinetically preferred reactive pathway for radical **10** with the five-membered nitrogen anion **7**, discrepancies were found with respect to the preferred C-site. While AM1[19] fails to differentiate the transition states (TSs) for C_2 and C_3-coupling (the most stable C–C radical anion formed by reaction at C_3), B3LYP points to C_2-substitution as the slightly preferred one ($\sim$1 kcal mol^{-1}) both at the TS and radical anion level (Fig. 3). From the three reactive positions, coupling at N, despite being less favoured kinetically, is the one that affords the most stable radical anion by either procedure in the gas phase.

The AM1 PES evaluation for imidazole anion **8** points to C_2 and C_4 as the preferred reactive sites with similar activation energies (Table 2). The difference in exothermicity between the C_4 and C_2-radical anions could be taken as indicative of the preferred reaction site, in agreement with experimental results.[10]

The B3LYP PESs were further improved by inclusion of the solvent effect evaluated through a continuum model. In the presence of methanol, as model protic solvent, the reactants of all the systems under consideration are more stabilised than

Table 2 Energy differences between relevant points of the potential energy surface (PES) for the reaction of phenyl radicals (**10**) with anions **1–9**

		AM1		B3LYP(6-31G*)		B3LYP(6-31G*) Continuum solvent[d]	
Anion	Position[a]	E_a [b]	ΔE_r [c]	E_a [b]	ΔE_r [c]	E_a [b]	ΔE_r [c]
1	**C_2**	−0.90	−40.50				
	C_4	0.76	−35.68				
	O	3.10	−21.95				
2	**C_1**	−0.26	−45.94	−8.01	−39.58	10.57	−20.61
	C_3	−0.27	−43.77				
	O	3.96	−29.57	−1.66	−24.84	25.36	3.31
3	C_1	2.41	−38.31				
	C_3	−0.23	−42.78				
	O	4.31	−28.76				
4	C_5	1.62	−37.55				
	N_1	3.11	−42.52				
5	C_5	2.23	−31.02				
	N_1	6.79	−25.58				
6	**C_5**	0.00	−37.84	−4.37	−25.27	9.60	−18.25
	N_1	6.75	−25.58	−0.24	−22.19	26.72	−1.79
7	**C_2**	−4.19	−35.39	−10.58	−27.12	15.53	−7.54
	C_3	−4.19	−40.27	−9.32	−25.10	16.05	−4.26
	N	4.32	−41.00	−8.58	−29.67	22.42	−6.70
8	**C_2**	0.85	−30.78				
	C_4	0.64	−35.72				
	N	5.04	−38.23				
9	C_2	1.41	−32.37				
	$C_{4(7)}$	1.00	−35.82				
	$C_{5(6)}$	0.79	−39.16				
	N	6.57	−33.06				

[a] Experimental preferred reaction sites indicated in bold. [b] E_a (kcal mol^{-1}) = energy difference between transition states and reactants (anion + phenyl radical). [c] ΔE_r (kcal /mol^{-1}) = reaction energy (energy difference between radical anion of product and reactants). [d] Continuum solvent model for methanol, without geometry optimization. Differences in total solution phase energies informed.

the TSs and the radical anions, as expected from the higher charge localization of the anion (see Fig. 1–3, Table S1, Fig. S2†). On this basis, all the reactions evaluated at the B3LYP level which have low or no activation energy in the gas phase transform into reactions with energy barriers in solution.

The TSs of these couplings are located early along the reaction coordinate and their gas phase energy ordering is maintained in the continuum solvent medium. Moreover, their energy difference increases and the C–C TSs are the ones that experience the higher stabilization.

The C–C route becomes thermodynamically preferred for all the anions under study including anion **7**, for which the N site gives the most stable intermediate in the gas phase.

In Fig. 4, the electrostatic potential maps evaluated for the C–C and C–O intermediates formed between radical **10** and anion **2** are presented. As shown in the figure, the C–C radical anion is the one that bears a higher negative charge localisation in the gas phase and as such it becomes the most stabilized in solution. Moreover, for this anion, O-coupling transforms into a slightly endothermic reaction in solution.

4-Nitrobenzyl radical

As seen from Table 1, FMO definitively fails to explain the regiochemistry of the reaction of anions **1**, **3**, and **8** with the stabilized 4-nitrobenzyl radicals (**11**); this methodology shows a similar reactivity pattern for both radical types, **10** and **11**.

Table 3 Energy differences between PES relevant points of the reaction of 4-nitrobenzyl radical (**11**) with different nucleophiles

		AM1		B3LYP(6-31G*)		B3LYP(6-31G*) Continuum solvent[d]	
Anion	Position[a]	E_a [b]	ΔE_r [c]	E_a [b]	ΔE_r [c]	E_a [b]	ΔE_r [c]
1	C_2	−5.57	−27.83	−20.31	−30.16	22.85	0.23
	O	−5.44	−29.82	−21.94	−32.40	21.78	−11.18
3	C_1	−0.40	−19.04				
	C_3	0.05	−23.46				
	O	−3.26	−25.07				
8	C_2	−4.36	−24.60	−20.82	−30.69	29.12	−4.36
	C_4	−7.16	−31.71	−21.50	−31.63	25.75	−2.88
	N	0.70	−36.36	−18.20	−42.39	20.91	−16.13
9	C_2	5.06	−11.55				
	N	4.67	−28.94				

[a] Experimental preferred reaction sites indicated in bold. [b] E_a (kcal mol^{-1}) = energy difference between transition states and reactants (anion + 4-nitrobenzyl radical). [c] ΔE_r (kcal mol^{-1}) = reaction energy (energy difference between radical anion of product and reactants). [d] Continuum solvent model for methanol, without geometry optimization. Differences in total solution phase energies informed.

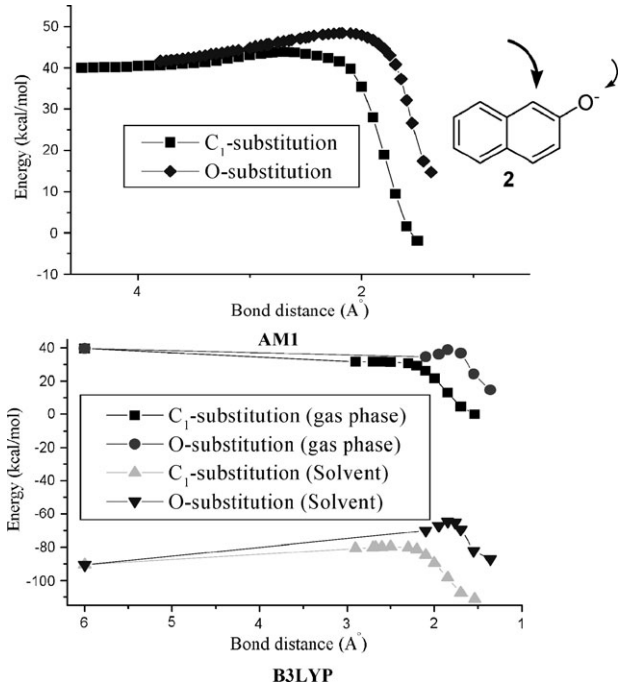

Fig. 1 Calculated PES, in the gas phase and in methanol, for the reaction of phenyl radicals at the C_1 and oxygen (O) sites of naphthoxide anion (**2**). All points in the B3LYP profile relative to the most stable gas phase radical anion taken as zero energy.

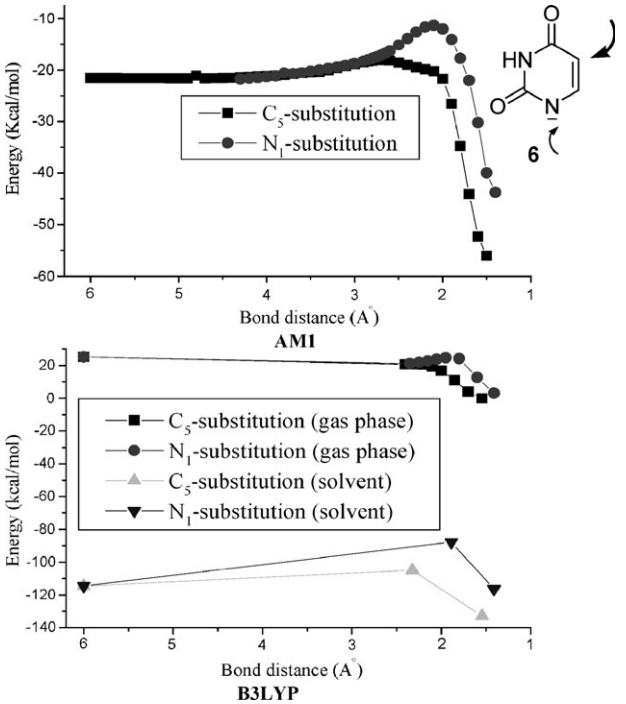

Fig. 2 Calculated PES, in the gas phase and in methanol, for the reaction of phenyl radicals at the C_5 and N_1 sites of uracil anion (**6**). All points in the B3LYP profile relative to the most stable gas phase radical anion taken as zero energy.

As previously mentioned, **11** reacts with anions **1**,[6] **3**,[5] **5**,[12] **8**[12] and **9**[12] to afford only heteroatom substitution.

Table 3 presents the energy of the PES stationary points evaluated for the reaction of **11** with oxyanions **1**, **3** and the heteroaryl nitrogen anions **8** and **9**.

At difference with phenyl radicals, the gas phase AM1 and B3LYP PESs calculated for the reaction of **11** with oxyanions **1–3** predicts the O-coupling surface to be slightly lower in energy ($\approx$2 kcal mol^{-1}) than the C-coupling one. This stabilization advantage maintains in the presence of a polar medium (Table 3).

The electrostatic potential maps evaluated for the C–C and C–O intermediates formed in the reaction of radical **11** with anion **1** are presented in Fig. 5. As seen in the figure, in the 4-nitrobenzyl system heteroatom-alkylation affords the radical anion with higher charge and spin localization, mainly located on the nitro group, a strong electron acceptor (see also Fig. S4†). On the basis of this electronic distribution the C–heteroatom radical anion becomes more stable than the C–C one. This behavior opposes the relative stability order obtained in the coupling with phenyl radicals. Moreover, the C–heteroatom intermediates experience higher stabilization in a polar medium and therefore C–heteroatom bond formation is the thermodynamically preferred route, not only in the gas phase but also in solution.

For the nitrogen anion **8**, and similarly to the oxyanions, B3LYP shows that C–N bond formation is preferred in solution both on kinetic and thermodynamic grounds.

The nitro group effect was further investigated by inspection of the PES for the reaction of anion **1** with 4-nitrophenyl radical (**12**). Table 4 shows the energy information for the

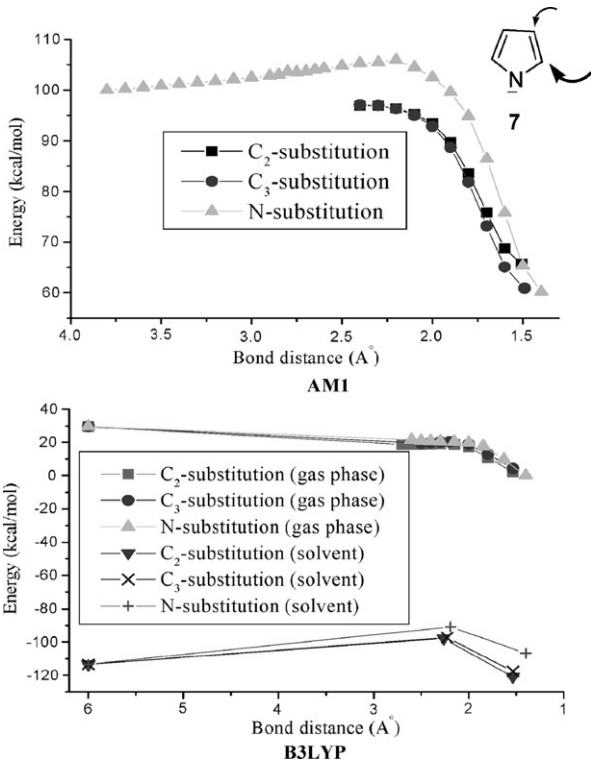

Fig. 3 Calculated PES, in the gas phase and in methanol, for the reaction of phenyl radicals at the C_2, C_3 and N sites of pyrrole anion (**7**). All points in the B3LYP profile relative to the most stable gas phase radical anion taken as zero energy.

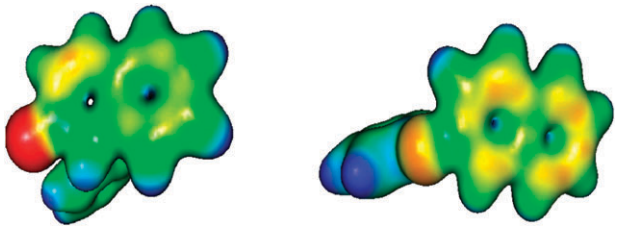

Fig. 4 Gas phase B3LYP electrostatic potential (from red (negative) to blue (positive)) for radical anions formed by reaction of phenyl radical at the C_1 (left) and O (right) sites of anion **2**.

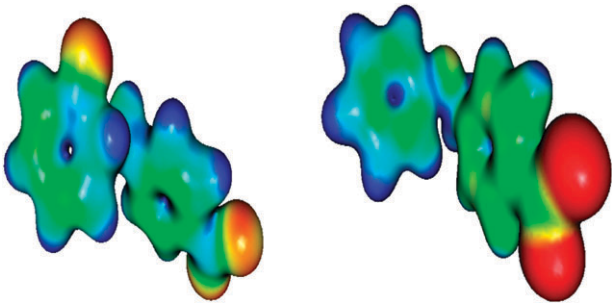

Fig. 5 Gas phase B3LYP electrostatic potential (from red (negative) to blue (positive)) for the radical anions formed by reaction of 4-nitrobenzyl radical (**11**) at the C_1 (left) and oxygen (right) sites of phenoxide anion (**1**).

main structures evaluated on this PES and its comparison with phenyl (**10**) and 4-nitrobenzyl radicals (**11**). As seen in the table, with 4-nitrophenyl radicals, like **11**, the C–O bond formation affords the most stable radical anion. However, in contrast with the behavior observed with **11**, bond formation at C_2 of the anion is pointed as its preferred kinetic route, in agreement with the experimental finding for the reaction of 4-$O_2NC_6H_4N_2SPh$ with anion **1** (70% C_2-substitution).[16]

In Fig. 6, the relevant geometric and electronic properties of the TSs for C- and O-coupling of radicals **11**, **12** with anion **1** and of radical **10** with anion **2** are presented.

As seen from the figure, the C–O (**a**) and C–C (**d**) TSs of the 4-nitrobenzyl radical show a similar spin distribution. However, the most stable C–O TS is characterized by a slightly higher spin on the nitrobenzyl moiety ($\approx$0.1 e^-) which resembles the spin distribution that characterizes the most stable C–O radical anion (see Fig. S4†).

In the coupling with phenyl radicals the most stable TS is the one that shows a spin distribution more similar to that of the most stable C–C radical anion (Fig. 6(**c**, **f**), Fig. S2†).

On the other hand, despite both TSs showing a similar spin distribution, in the 4-nitrophenyl case, the distribution of the higher energy O–C TS opposed that of the radical anion it will form (Fig. 6(**b**, **e**), Fig. S5†).

The most stable C–C TSs of the phenyl and 4-nitrophenyl radicals are intramolecularly stabilized by electrostatic interactions between the heteroatom and the $hydrogen_\beta$ of the radical centre (Fig. 6(**b**, **c**)). Moreover, in these TSs the heteroatom is more exposed to a solvent medium (compare structures **b**–**c** and **e**–**f**, Fig. 6). Thus, due to solvent and intramolecular effects, the gas phase energy ordering is maintained in solution and the C–C route is the kinetically preferred one.

With the 4-nitrobenzyl radical on the other hand, the gas phase C–O TS, slightly more stable than the C–C one, is extra-stabilized by intramolecular electrostatic interactions of the heteroatom with the hydrogens of the $C_{radical}$ centre (Fig. 6(**a**)).

Despite in the C–C TS the oxygen is more exposed to the solvent and it becomes more stabilized in a polar medium (Fig. 6(**d**), Table S1†); this stabilization does not suffice to modify the C–O higher stability and the latter is maintained as the minimum energy reaction path in a continuum polar medium for the 4-nitrobenzyl case.

Conclusions

From the theoretical study presented here we conclude that the main experimental outcome of these reactions is kinetically determined. In the reaction of anions **1–8** with phenyl radicals, C–C coupling is the preferred pathway on kinetic and thermodynamic grounds; the exception being the reaction of anion **1** with 4-nitrophenyl radicals for which C–C is preferred kinetically, while C–O leads to the most stable intermediate. Experimentally only C-coupling was observed with this radical.

For the 4-nitrobenzyl radical, an energy advantage is calculated for the C–heteroatom route which is slightly higher for the oxyanion **1**. Spin distribution and electrostatic interactions between the heteroatom and the hydrogens of the radical centre seem to play a stabilizing role for these TSs.

The B3LYP functional with inclusion of solvent is recommended to obtain the correct energy potential surfaces of these systems. However, in most cases, the gas phase energy

Table 4 Energy differences between relevant points of the PES for the reaction of anion **1** with different radicals

		AM1		B3LYP(6-31G*)		B3LYP(6-31G*) Continuum solvent[d]	
Radical	Position[a]	E_a[b]	ΔE_r[c]	E_a[b]	ΔE_r[c]	E_a[b]	ΔE_r[c]
10	**C_2**	−0.90	−40.50				
	O	3.40	−21.95				
11	C_2	−5.57	−27.83	−20.31	−30.16	22.85	0.23
	O	−5.44	−29.82	−21.94	−32.40	21.78	−11.18
12	**C_2**	−9.16	−27.11	−21.29	−52.59	15.51	−26.91
	O	−5.38	−30.89	−20.88	−59.95	19.53	−43.23

[a] Experimental preferred reaction sites indicated in bold. [b] E_a (kcal mol^{-1}) = energy difference between transition states and reactants (anion + radical). [c] ΔE_r (kcal mol^{-1}) = reaction energy (energy difference between radical anion of product and reactants). [d] Continuum solvent model for methanol, without geometry optimization. Differences in total solution phase energies informed.

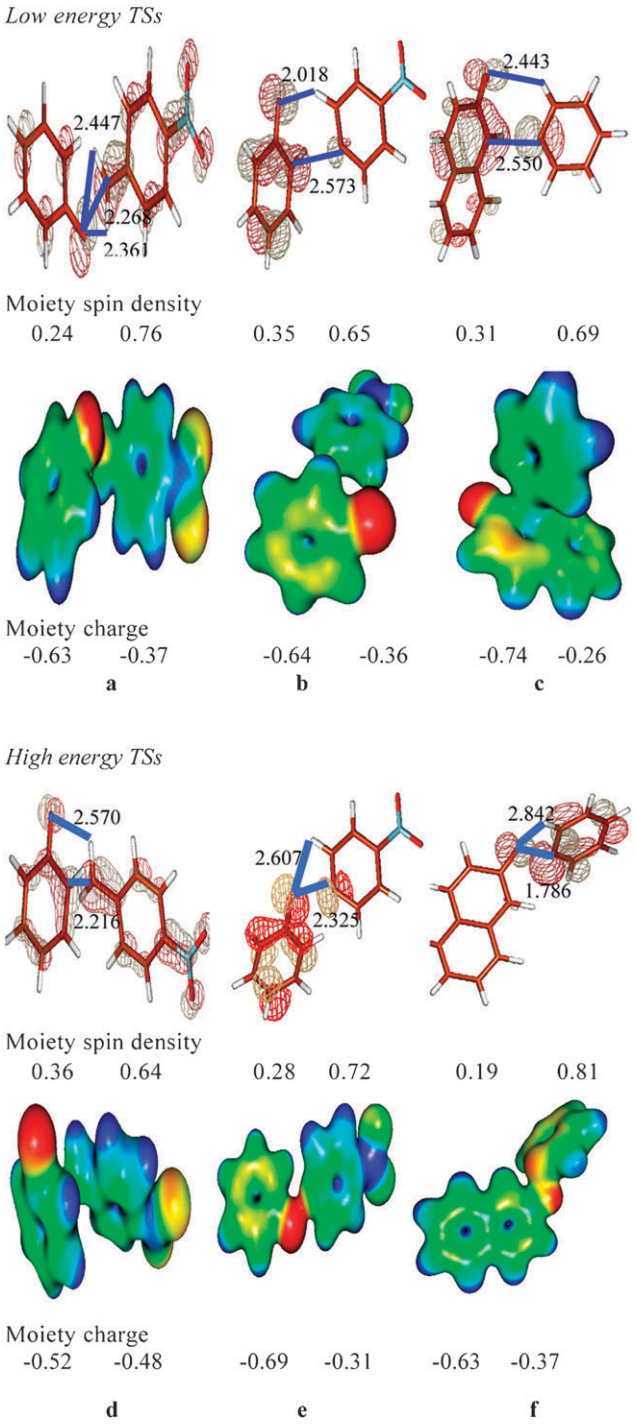

Fig. 6 Unpaired spin distribution and gas B3LYP electrostatic potential of TSs for reaction of oxyanion **1** with radicals **11** and **12** (a, b, d, e) and oxyanion **2** with radical **10** (c, f).

ordering calculated for the TSs is maintained in solution and therefore B3LYP gas phase calculations can be performed to predict the experimental outcome of the coupling of different anions with radicals. Care should be taken in the use of AM1 to study these reactions with nitrogen heteroaryl anions.

FMO studies can be helpful with phenyl radical but not with radicals for which steric and/or electrostatic interactions are not accounted for by this approach.

Computational procedure

The system was studied with the AM1 semiempirical method,[20] as implemented in the Gaussian 98 package of programs[21] and the B3LYP[22] DFT[23] functional, as implemented in the Jaguar[24] and Gaussian[21] programs within the UHF or RHF formalism for open and closed shell species respectively, to properly account for their electronic nature. First, the most stable conformers of the radical anions $RNu^{-\bullet}$ were evaluated through an AM1 conformational search by scanning the two or three main torsion angles (for an example, see Fig. S1†). The conformers thus obtained were then refined with complete geometry optimization. The geometries thus found were used as starting points to study the PES corresponding to the C–C or C–heteroatom bond breaking/formation. The transition states located through the reaction coordinate method were then refined and characterized by Hessian matrix calculations: all positive eigenvalues corresponding to a minimum and one imaginary frequency to a transition state structure.[25]

PES explorations within the B3LYP DFT functional and the 6-31G* basis set were carried out by the same procedure. Zero point energy corrections were performed at the B3LYP/6-31G* level. Similar results were obtained either with this basis set or the 6-31 + G* basis set (see Table S2†).

The charge localization was obtained by Mulliken population analysis. The solvent effect was modelled with a continuum model[26] as implemented in the Jaguar program, choosing methanol as model polar solvent (model solvent methanol: dielectric constant = 33.62, probe radius (r_p) = 2.00196 Å).[27] The solvent stabilization was evaluated from single point calculations on the gas phase optimized geometries at the B3LYP/6-31G* theory level; electrostatic and non-electrostatic contributions being considered.

Acknowledgements

This work was supported by the Agencia Córdoba Ciencia (ACC), Consejo Nacional de Investigaciones Científicas y Técnicas (CONICET) and Secretaría de Ciencia y Tegnología (SECyT), Universidad Nacional de Córdoba, Argentina. G.A.B. thanks CONICET for the award of a fellowship.

References

1 (*a*) R. A. Rossi, A. B. Pierini and A. B. Peñéñory, *Chem. Rev.*, 2003, **103**, 71–167; (*b*) R. A. Rossi, A. B. Pierini and A. N. Santiago, in *Organic Reactions*, ed. L. A. Paquette and R. Bittman, Wiley, New York, 1999, pp. 1–271.
2 (*a*) R. Beugelmans and M. Bois-Choussy, *J. Org. Chem.*, 1991, **56**, 2518–2522; (*b*) A. B. Pierini, M. T. Baumgartner and R. A. Rossi, *Tetrahedron Lett.*, 1988, **29**, 3451–3454; (*c*) R. Beugelmans and J. Chastanet, *Tetrahedron*, 1993, **49**, 7883–7890; (*d*) C. Combellas, C. Suba and A. Thiébault, *Tetrahedron Lett.*, 1994, **35**, 5217–5220.
3 N. Alam, C. Amatore, C. Combellas, J. Pinson, J.-M. Savéant, A. Thiébault and J. N. Verpeaux, *J. Org. Chem.*, 1988, **53**, 1496–1504.
4 M. T. Baumgartner, T. C. Tempesti and A. B. Pierini, *Arkivoc*, 2003, **part X**, 420–433.
5 N. Kornblum, L. Cheng, T. M. Davies, G. W. Earl, N. L. Holy, R. C. Kerber, M. M. Kestner, J. W. Manthey, M. T. Musser, H. W. Pinnick, D. H. Snow, F. W. Stuchal and R. T. Swiger, *J. Org. Chem.*, 1987, **52**, 196–204.
6 N. Kornblum, *Angew. Chem., Int. Ed. Engl.*, 1975, **14**, 734–745.
7 A. B. Pierini, M. T. Baumgartner and R. A. Rossi, *Tetrahedron Lett.*, 1987, **28**, 4653–4656.

8 T. C. Tempesti, A. B. Pierini and M. T. Baumgartner, *J. Org. Chem.*, 2005, **70**, 6508–6511.
9 M. Chahma, C. Combellas and A. Thiébault, *Synthesis*, 1994, 366–368.
10 M. Chahma, C. Combellas and A. Thiébault, *J. Org. Chem.*, 1995, **60**, 8015–8022.
11 M. Medebielle, M. A. Oturan, J. Pinson and J.-M. Savéant, *J. Org. Chem.*, 1996, **61**, 1331–1340.
12 (*a*) R. Beugelmans, A. Lechevalier, D. Kiffer and P. Maillos, *Tetrahedron Lett.*, 1986, **27**, 6209–6212; (*b*) R. Benhida, T. Gharbaoui, A. Lechevallier and R. Beugelmans, *Nucleosides Nucleotides*, 1994, **13**, 1169–1177.
13 J. M. Saveant, *J. Phys. Chem.*, 1994, **98**, 3716–3724.
14 In the second order perturbation ($\varepsilon'' = (c_{Hi}c_{Sj}\beta_{ij})^2/(E_{HOMO} - E_{SOMO})$), c_{Hi} is the coefficient of the atomic orbital (AO) of atom i in the HOMO of the nucleophile. The term c_{Sj} is the coefficient of the AO of radical j in the SOMO. β_{ij} is the resonance integral between atoms i and j. $\beta_{CO} = 3.77$ eV. $\beta_{CC} = 5$ eV. $\beta_{NC} = 4.35$ eV: (*a*) N. K. Houk, J. Sims, R. E. Duke, R. W. Strozier and J. K. George, *J. Am. Chem. Soc.*, 1973, **95**, 7287–7301; (*b*) N. K. Houk, J. Sims, C. R. Watts and L. J. Luskus, *J. Am. Chem. Soc.*, 1973, **95**, 7301–7315.
15 The preferred coupling site will be the atom bearing the largest HOMO coefficient whenever the differences in β_{ij}, the resonance integral between atoms i and j involved in the two types of bond formation, do not suffice to modify the coefficient tendency (see eqn (7)).
16 G. Petrillo, M. Novi, C. Dell'Erba, C. Tavani and G. Berta, *Tetrahedron*, 1990, **46**, 7977–7990.
17 M. Medebielle, M. A. Oturan, J. Pinson and J. M. Saveant, *Tetrahedron Lett.*, 1993, **34**, 3409–3412.
18 C. Z. Xia, Z. B. Chen and Z. Zhang, *Chin. Chem. Lett.*, 1991, **2**, 429–432.
19 Note that the AM1 method fails in the evaluation of thermodynamic and geometric properties of pyrrole (see ref. 20).
20 M. J. S. Dewar, E. G. Zoebisch, E. F. Healy and J. P. Stewart, *J. Am. Chem. Soc.*, 1985, **107**, 3902–3909.
21 M. J. Frisch, G. W. Trucks, H. B. Schlegel, G. E. Scuseria, M. A. Robb, J. R. Cheeseman, V. G. Zakrzewski, J. A. Montgomery, Jr., R. E. Stratmann, J. C. Burant, S. Dapprich, J. M. Millam, A. D. Daniels, K. N. Kudin, M. C. Strain, O. Farkas, J. Tomasi, V. Barone, M. Cossi, R. Cammi, B. Mennucci, C. Pomelli, C. Adamo, S. Clifford, J. Ochterski, G. A. Petersson, P. Y. Ayala, Q. Cui, K. Morokuma, D. K. Malick, A. D. Rabuck, K. Raghavachari, J. B. Foresman, J. Cioslowski, J. V. Ortiz, A. G. Baboul, B. B. Stefanov, G. Liu, A. Liashenko, P. Piskorz, I. Komaromi, R. Gomperts, R. L. Martin, D. J. Fox, T. Keith, M. A. Al-Laham, C. Y. Peng, A. Nanayakkara, C. Gonzalez, M. Challacombe, P. M. W. Gill, B. G. Johnson, W. Chen, M. W. Wong, J. L. Andres, M. Head-Gordon, E. S. Replogle and J. A. Pople, *GAUSSIAN 98 (Revision A.7)*, Gaussian, Inc., Pittsburgh, PA, 1998.
22 (*a*) C. Lee, W. Yang and R. G. Parr, *Phys. Rev. B*, 1988, **37**, 785; (*b*) A. D. Becke, *Phys. Rev. A*, 1988, **38**, 3098; (*c*) B. Miehlich, A. Savin, H. Stoll and H. Preuss, *Chem. Phys. Lett.*, 1989, **157**, 200.
23 (*a*) P. Hohenberg and W. Kohn, *Phys. Rev.*, 1964, **136**, B864; (*b*) W. Kohn and I. J. Sham, *Phys. Rev.*, 1965, **140**, A1133.
24 *Jaguar, version 6.0*, Schrödinger L.L.C., New York, NY, 2005. See, http://www.schrodinger.com.
25 J. W. McIver and A. Komornicki, *J. Am. Chem. Soc.*, 1972, **94**, 2625.
26 (*a*) D. J. Tannor, B. Marten, R. Murphy, R. A. Friesner, D. Sitkoff, A. Nicholls, M. Ringnalda, W. A. Goddard and B. Honig, *J. Am. Chem. Soc.*, 1994, **116**, 11875; (*b*) B. Marten, Kim, C. Cortis, R. A. Friesner, R. B. Murphy, M. Ringnalda, D. Sitkoff and B. Honig, *J. Phys. Chem.*, 1996, **100**, 11775.
27 The solvent is represented as a polarizable continuum (with dielectric constant ε) surrounding the molecular complex at an interface constructed by combining atomic van der Waals radii with the effective probe radius of the solvent. Charges are allowed to develop on this interface according to the electrostatic potential of the solute and ε, then the polarized reaction field of the solvent acts back on the quantum mechanical description of the solute. The wave function of the complex is relaxed self-consistently with the reaction field to solve the Poisson–Boltzmann (PB) equations. The solvent was represented with the following parameters: dielectric constant and probe radius. For examples of use of the model see: (*a*) J. G. Uranga, D. M. A. Vera, A. N. Santiago and A. B. Pierini, *J. Org. Chem.*, 2006, **71**, 6596–6599; (*b*) J. J. Klicic, R. A. Friesner, S. Y. Liu and W. C. Guida, *J. Phys. Chem. A*, 2002, **106**, 1327–1335; (*c*) V. S. Bryantsev, M. S. Diallo and W. A. Goddard III, *J. Phys. Chem. A*, 2007, **111**, 4422–4430; (*d*) R. J. Nielsen, J. M. Keith, B. M. Stoltz and W. A. Goddard III, *J. Am. Chem. Soc.*, 2004, **126**, 7967–7974.